DOCU

NASA Contractor Report 156857

Estimation of the Ocean Geoid Near the Biake Escarpment Using GEOS-3 Satellite Altimetry Data

(NASA-CR-156857) ESTIMATICN OF THE OCEAN GEOID NEAR THE ELAKE ESCARFMENT USING GEOS-3 SATELLITE ALTIMETRY (Analytic Sciences Corp.) 34 p HC A03/MF A01 CSCL 08G

N79-30868

Unclas

G3/46 31821

Robert F. Brammer

August 1979

National Aeronautics and Space Administration

Wallops Flight Center
Wallops Island, Virginia 23337
AC 804 824-3411

NASA Contractor Report 156857

Estimation of the Ocean Geoid Near the Blake Escarpment Using GEOS-3 Satellite Altimetry Data

Robert F. Brammer
The Analytic Sciences Corporation
Six Jacob Way
Reading, MA 01867

Prepared Under Contract No. NAS6-2476

NASA
National Aeronautics and
Space Administration

Wallops Flight Center
Wallops Island, Virginia 23337
AC 804 824-3411

TABLE OF CONTENTS

LIST OF FIGURES

LIST OF TABLES

1. INTRODUCTION

The primary objective of this study was to determine the feasibility of measuring local geoid undulations and deflections of the vertical with high accuracy using satellite radar altimeters. This determination was made by processing the GEOS-3 altimeter data, estimating the local undulations and deflections using optimal Kalman smoothing and related techniques, and by comparing the results with independently derived geoidal estimates obtained by the U.S. Naval Oceanographic Office (NAVOCEANO) from surface shipboard gravimetric measurements. This comparison resulted in a statistical summary (mean and rms differences) along individual tracks of data. In general, the results of comparing these geoid undulation estimates showed a mean difference of two to three meters and an rms difference of 20 to 40 cm. For the vertical deflections, the mean differences were not significant, except for those tracks affected by the western edge of the Gulf Stream. The rms differences were typically between one and two $\widehat{\sec}$. (arc seconds).

An additional objective was to determine the limits of the capability of the altimeter to resolve short wavelength features in the geoid. This analysis was based on a cross spectrum study of closely spaced parallel subtracks which are essentially parallel lines over limited geographical regions. The results of this analysis show that the altimeter can easily resolve geoid wavelengths of 100 km, and the lower limit varies from 30 km to 80 km, depending on several factors described in this paper.

The analysis was performed using data collected in the region of the Blake Escarpment. This area was selected for several reasons. The first reason is the availability of high resolution surface data produced from shipboard gravimetric surveys with which the results of the satellite data processing can be compared. Second, the Blake Escarpment region is an interesting region geophysically, and the gravity disturbances are such that the vertical deflections range from very small (2 to 5 $\widehat{\text{sec}}$.) in part of the region, to very large in other parts (nearly 40 $\widehat{\text{sec}}$.). Third, this area is partially within the GEOS-3 calibration area in which it was anticipated that orbits and tide height corrections would be most accurate. The geographic locations of the data collection area and the Blake Escarpment, are shown in Fig. 1-1, and the east vertical deflection at 28 degrees latitude derived from the NAVOCEANO data is shown in Fig. 1-2.

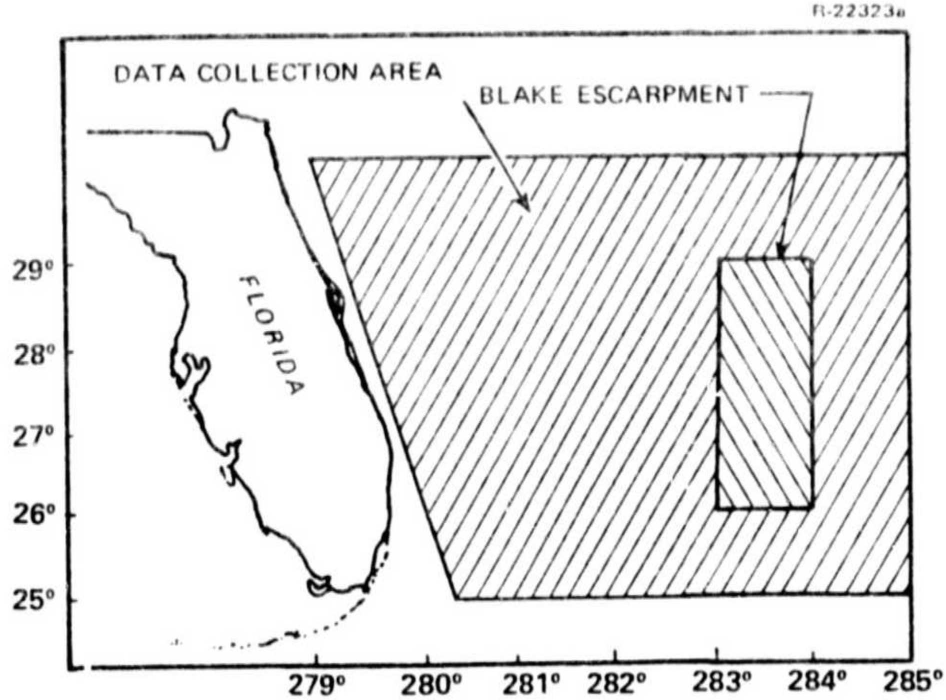

Figure 1-1 Area of GEOS-3 Data Collection Used in This Study

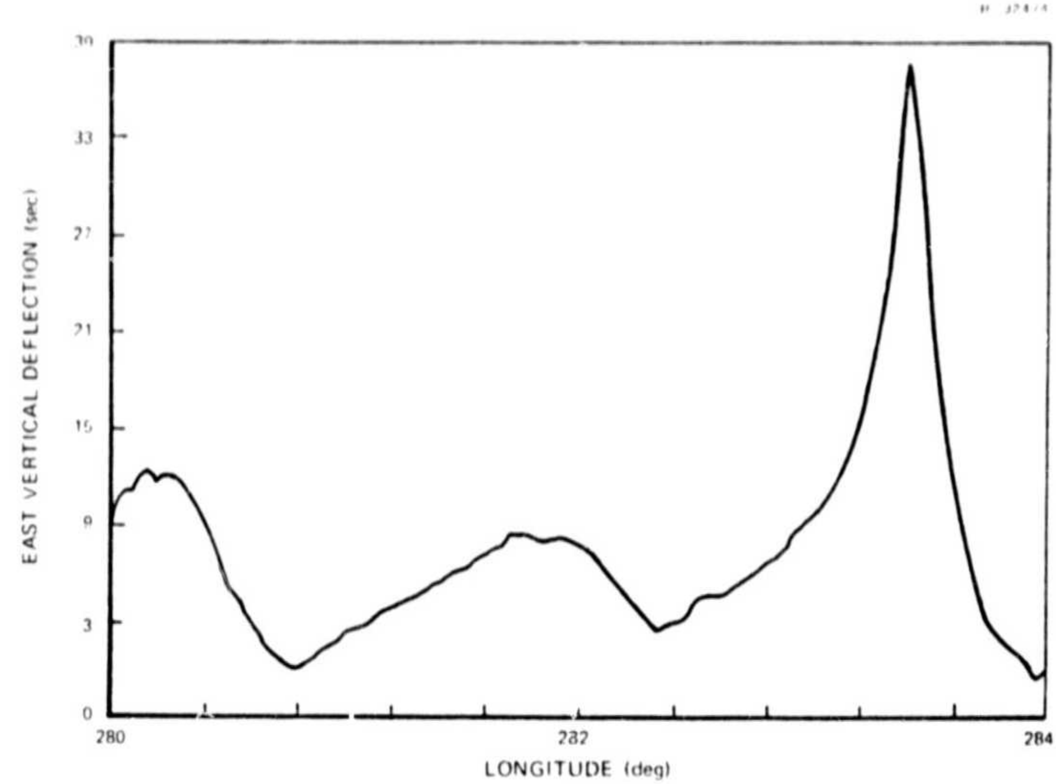

Figure 1-2 Gravimetrically-Derived East Vertical Deflection at 28 Degree North Latitude

This report is organized as follows. Chapter 2 describes the GEOS-3 data analyzed in this study and the data preprocessing required prior to data analysis. The geoid modeling and results are given in Chapter 3. The spectrum analysis and results of the altimeter resolution study are presented in Chapter 4. Chapter 5 contains a summary of the principal conclusions of the study.

2. GEOS-3 ALTIMETRY DATA AND DATA PREPROCESSING

2.1 DATA USED IN THIS STUDY

The data used in this study for all the geoid estimation and geoid resolution results described here were the sea surface height values computed along the altimeter subtracks. These values were computed by NASA/WFC and supplied on the investigators' data tapes. Consideration was given only to the intensive mode data, since it was shown early in the study (Ref. 1) that the global mode data was not sufficiently accurate to meet the above objectives. All processing was performed on data sets taken at the rate of ten samples per second.

As described in Chapter 1, the analysis was to be performed on data taken in the vicinity of the Blake Escarpment. This constraint resulted in a set of approximately 75 tracks available for processing. For the purposes of this paper, a subset of these tracks has been selected to illustrate the results. The orbit numbers, start and stop times are given in Table 2.1-1, and the subtracks are shown in Fig. 2.1-1. Note that the tracks are grouped in sets of two or three parallel tracks.

The near repeatability of the tracks is an important aspect of the GEOS-3 data set. Since the spacing between the subtracks (1 to 3 km) is often less than the altimeter beam spot size (3.6 km), these tracks often contain overlapping regions sampled at time intervals of a few months. This subtrack repeatability can be exploited in many ways to

TABLE 2.1-1

SELECTED GEOS-3 DATA

T-1919

ORBIT NO	SEGMENT START TIME				SEGMENT STOP TIME			
	YEAR	MONTH	DAY	SEC. OF DAY (GMT)	YEAR	MONTH	DAY	SEC. OF DAY (GMT)
1178	75	07	02	23044.894854	75	07	02	23149.65529
1306	75	07	11	27133.903559	75	07	11	27238.663997
1505	75	07	25	32857.498202	75	07	25	32962.258640
1682	75	08	06	74956.785739	75	08	06	75061.546178
1810	75	08	15	79027.360603	75	08	15	79134.169144
2031	75	08	31	48387.241886	75	08	31	48492.00243
2080	75	09	04	22.200872	75	09	04	74.529888
2208	75	09	13	4086.631075	75	09	13	4193.439615
2236	75	09	22	8155.157378	75	09	22	8259.917816
2358	75	09	23	58197.794426	75	09	23	58320.554864
2606	75	10	11	15549.997104	75	10	11	15602.326120
2756	75	10	21	69636.480681	75	10	21	69744.241119
2862	75	10	29	23681.007603	75	10	29	23785.768041
2884	75	10	30	73723.542241	75	10	30	73828.30267
3280	75	11	26	35134.030580	75	11	26	35238.79108

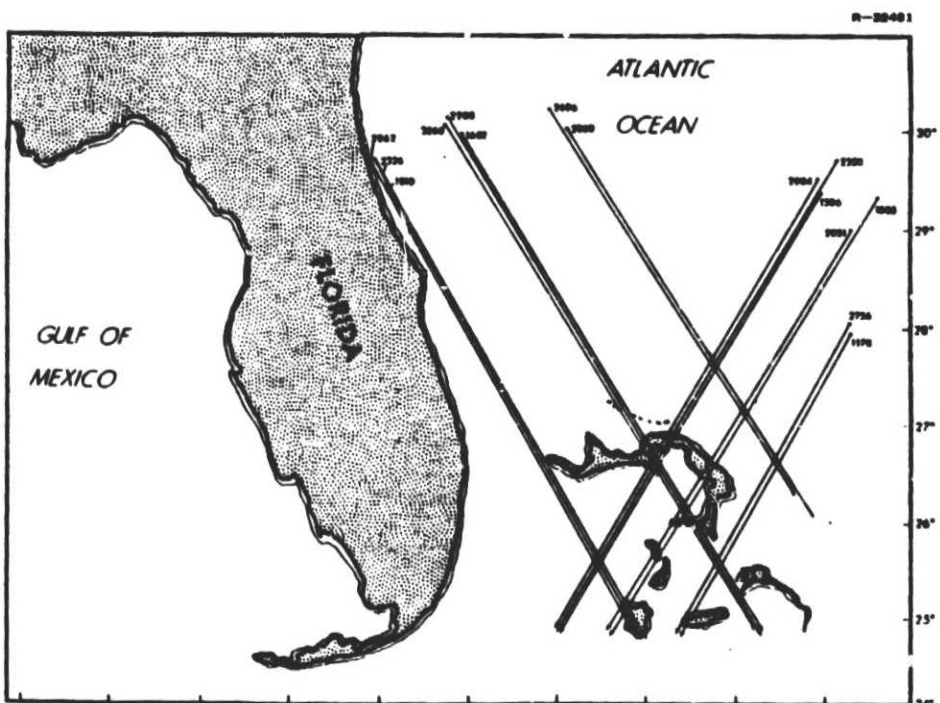

Figure 2.1-1 Selected Tracks of GEOS-3 Altimeter Data

analyze the GEOS-3 data. A method for performing this analysis is given in Chapter 4.

2.2 RAW DATA PREPROCESSING

For the purposes of this study, "raw data" is the sea surface height data sampled at the rate of ten per second. As received from NASA, the data were corrected for tropospheric refraction. Other corrections, however, were needed before the geoid estimation could be performed. This processing can be summarized as follows:

$$\begin{aligned}\text{Raw geoid estimate} = {} & \text{Sea Surface Height} \\ & - \text{Altimeter Bias} \\ & - \text{Tide Correction}\end{aligned} \tag{2.2-1}$$

The altimeter bias value was taken to be 5.3 meters as given in (Ref. 2). The tide model employed was that developed by Mofjeld for the GEOS-3 calibration area (Ref. 3). An ellipsoid conversion was also needed to transform the Navy geodetic values from the reference ellipsoid used by the Navy in referencing their surface gravimetric survey data. In the area of the Blake Escarpment, this ellipsoid conversion was 9.8 meters. Over the geographically limited region of the Blake Escarpment these corrections are nearly constant, and, thus, do not affect the estimation of the vertical deflections but only the absolute level of the geoid estimate.

The above corrections are routine and presented no difficulties in the study. However, another aspect of the preprocessing could not be handled in a routine manner. This aspect results from the presence of short term "spikes" in the data. These spikes are usually negative-going with magnitudes of several meters and time duration between

0.5 sec. to 0.9 sec. Often the spikes have magnitudes of approximately three, six or nine meters, but this is not universally true, nor are the spikes always negative.

The cause of these spikes is not known at present, but a study of those passes which contain a significant number suggests that the cause may be related to relatively high altitude rates or to the presence of short wavelength features in the geoid. However, the observed altitude rates apparently need not be large compared to the altimeter specification for altitude rate in order for spikes to occur. Though the spikes are believed to be induced by the altimeter and not by the ocean surface, the effect is often qualitatively highly repeatible. Two tracks which illustrate these phenomena are shown in Fig. 2.2-1. These tracks are within three km of each other as indicated in Fig. 2.1-1.

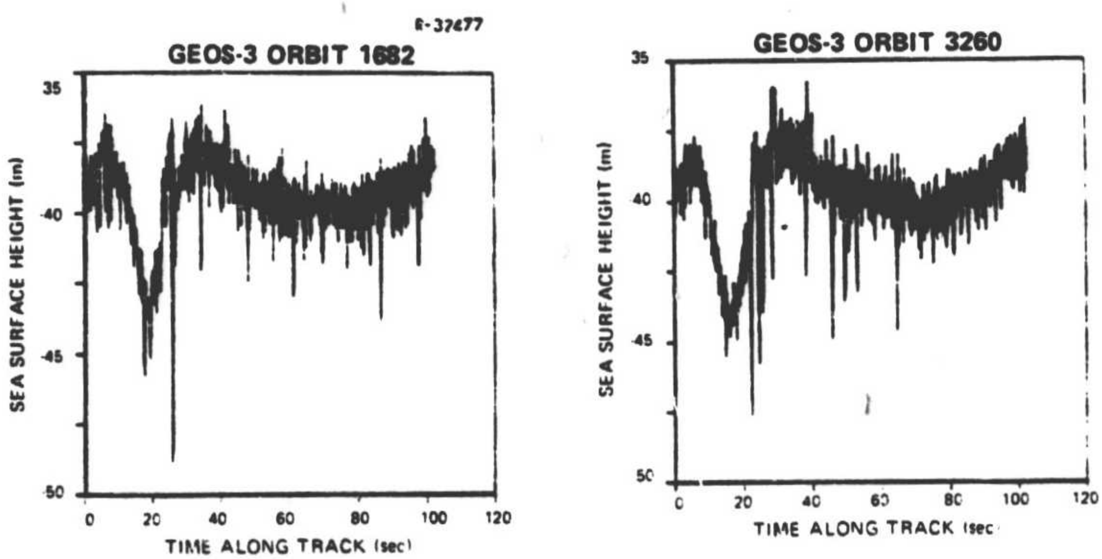

Figure 2.2-1 GEOS-3 Tracks Showing Short-Term Data Spikes

Before any of the processing to estimate geoid undulations and vertical deflections or to estimate spectra can be performed, the invalid data must be eliminated. Invalid data may result from spikes, over-land or nearly over-land subtracks, or altimeter loss of lock. Several approaches to automatic editing were tried, and the approach yielding the most satisfactory results involved a spike detecting algorithm based on comparing the difference between the raw data and a smoothed version of the data with a threshold level derived from the altimeter noise level. In this case, the smoothing filters employed were finite impulse response filters (Ref. 4), having a low pass characteristic. The finite impulse response filters used for this smoothing application were midpoint filters of the form

$$\overline{X}_i = \sum_{j=i-N}^{i+N} W_j X_j \qquad (2.2\text{-}2)$$

A 51 point filter was found to be satisfactory for this application. The filter weights, W_j, were chosen to provide the appropriate pass band. This pass band was derived from spectrum analysis of the data. Though, in practice, a certain amount of iteration was required to obtain satisfactory performance, a filter cut-off of 15 km was sufficient to edit the spikes without distorting the data. Of course, the optimal smoothers provide further smoothing. Results of the editing process (including mean removal) are shown in Fig. 2.2-2.

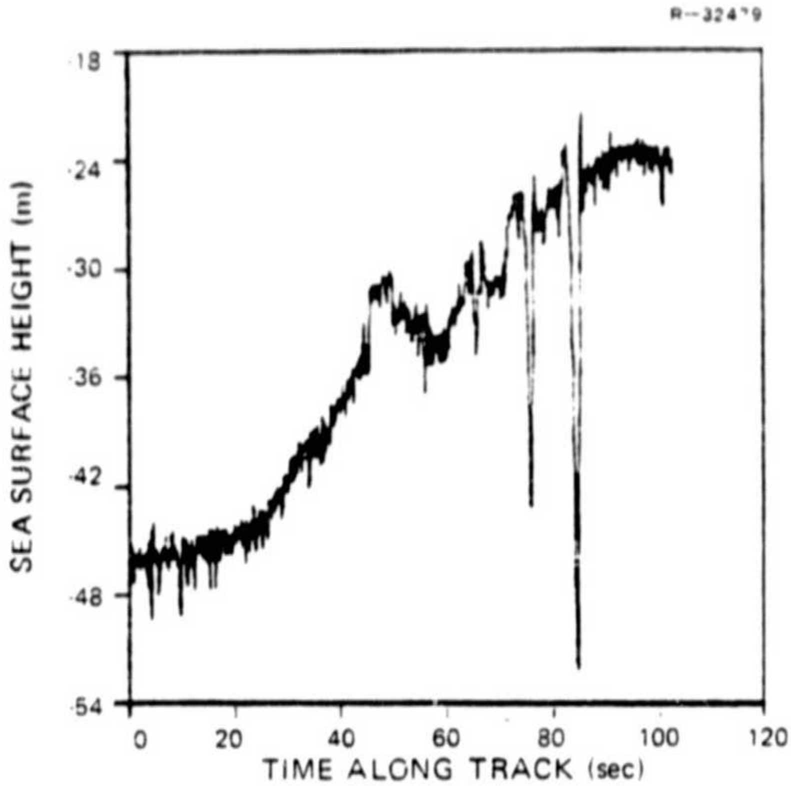

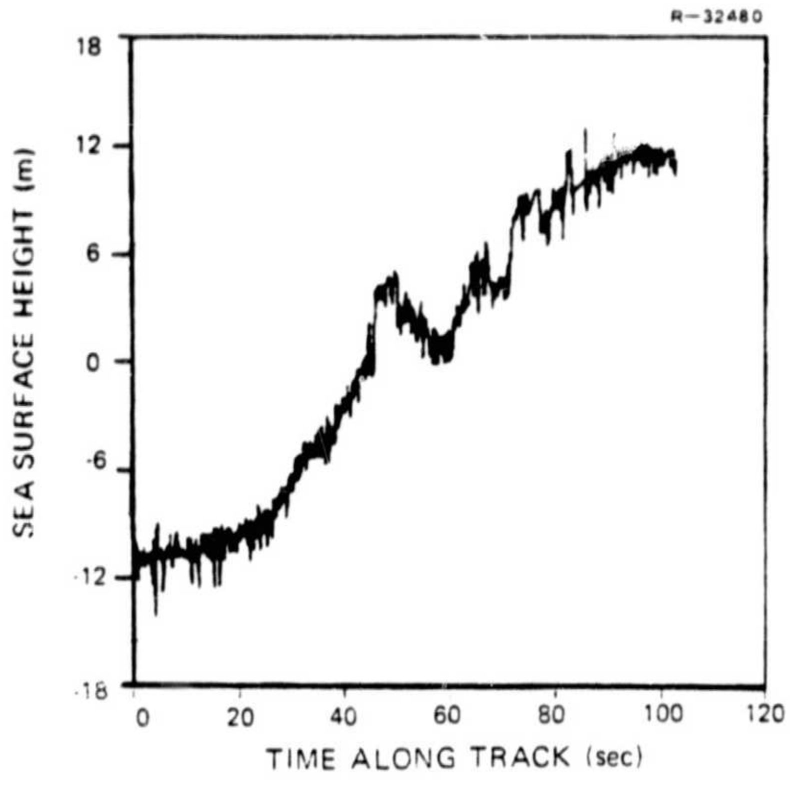

Figure 2.2-2 Illustration of GEOS-3 Altimeter Data Editing

3. GEOID ESTIMATION

3.1 GEOID MODELING

The altimeter data processing performed in this study relies on various assumed mathematical models for the variation in the sea surface height data along individual tracks. Some of the analysis used models that are explicitly parametric. These include the state space models used for optimal Kalman smoothing as well as the finite impulse response filters derived from various spectral passband shapes. Both of these techniques were used in the estimation of geoid undulations and vertical deflections. Other techniques used in data analysis were not parametric. These types include some of the spectrum analysis (e.g. FFT techniques) to be described in Section 4.2. Even though the techniques are nonparametric, the interpretation of the results still requires some type of model. This will be discussed further in Section 4.1.

One class of mathematical models used in this study to estimate the geoid is that of state space models (Ref. 5). These have the form

$$\dot{\underline{x}} = F\,\underline{x} + G\underline{w} \tag{3.1-1}$$

$$\underline{z} = H\,\underline{x} + \underline{v} \tag{3.1-2}$$

In this particular application the vector process, $\underline{x}$, models the geoid variations with particular components representing the geoid undulation and the along-track component of the vertical deflection. An example of such a model for geodetic applications is the TASC third order model described in (Ref. 6). The statistics of the process $\underline{x}$ are determined by the matrices F, G, and Q. The vector process, $\underline{z}$, is the measurement data corrupted by additive noise $\underline{v}$. In this application the measurements are the scalar sea surface heights following the preprocessing described in Chapter 2.

Some subtracks contain a large amount of long wavelength energy. This is particularly true for those passes going directly over the Escarpment. This energy must be removed using a trend removal algorithm before smoothing with a stationary model like the above TASC model. An alternative procedure which proved satisfactory is to augment the state vector with non-stationary trend states (e.g. first or second order polynomial dynamics) which can also be estimated. The ability to handle nonstationary states is one advantage (along with computational efficiency) of the Kalman smoothing approach with respect to classical filtering and smoothing techniques.

The TASC third order model requires the specification of undulation rms (σ_N) and correlation distance (c_N). To obtain best results, these parameters were estimated from a preliminary spectrum analysis following linear or quadratic trend removal. Typically, the values obtained for σ_N were between two and five meters with correlation distances between 60 km and 100 km.

An alternative modeling approach employed in this study was to fit autoregressive models of the form

$$x_n = A_1 x_{n-1} + \dots + A_k x_{n-k} + w_n \qquad (3.1\text{-}3)$$

where

- x_n is the undulation at position (or time) n along the track
- w_n is a random driving noise term (white noise with variance σ or covariance matrix P for a vector process)

- the parameters (matrices for vector processes), A_j and the order, k, are to be estimated from the data

The matrices, A_j, were estimated using the maximum entropy technique (Ref. 7). The approach used for the selection of the model order, k, was based on the final prediction error (Ref. 8). The model developed using this approach can be rewritten to form a discrete-time state space model which can then be used to apply the optimal Kalman smoothing algorithm. Generally, the optimum order selected for the tracks considered in this study was between five and twelve, and a seventh or eighth order model would often produce satisfactory results.

These alternative approaches did not generally produce significantly different geoid estimates for those tracks relatively free of invalid data. Comparisons among these various approaches and with other organizations performing similar analyses (Ref. 9), showed undulation estimate differences of between 10 cm and 30 cm and vertical deflection estimate differences of less than 0.5 $\widehat{\text{sec}}$. Such differences are not statistically significant within the accuracy of the data.

3.2 GEOID UNDULATION ESTIMATION RESULTS

This section presents typical results of the geoid undulation estimation results. As described in Chapter 1, these estimates were compared to the undulation estimates produced by the U.S. Navy using gravimetric survey data. The results are also compared to the NASA GEOS-3 calibration area geoid (Ref. 10). Over a typical track, the mean difference between the undulations estimated from the GEOS-3 data, and those estimated from the Navy data is about two to three meters. This is believed to be due primarily to GEOS-3 radial orbit uncertainties, but other long wavelength error sources could also be contributing. These may include long wavelength errors in the Navy geoid, tide model errors, errors in calibrating the altimeter bias, propagation uncertainties, etc. The rms difference is generally on the order of 20 cm to 30 cm showing that the altimeter does well in recovering the short wavelength (50 km - 200 km) features defined by the gravimetric data near the Blake Escarpment. It should be emphasized that the gravimetric undulations are also smoothed as a result of the Stoke's equation.

The results are illustrated in Fig. 3.2-1 which shows the results obtained for Rev. 2606. The 5.3 meter bias described earlier has not been subtracted from the altimeter data in order to display the data more clearly. These results were obtained using the TASC third order model described in Section 3.1 with parameters $\sigma_N = 3\text{m}$, $C_N = 80$ km (Ref. 6) and the altimeter noise, $\sigma_A = 60$ cm (at a sampling rate of 10/sec). This model has the form of Eqs. 3.1-1 and 3.1-2. The state vector, $\underline{x}$, is three-dimensional with components $\{x_j\}$. For this case the matrices F, G, Q, H, and R are defined as follows

$$F = \begin{pmatrix} -\beta & 0 & 0 \\ 1 & -\beta & 0 \\ 0 & 1 & -\beta \end{pmatrix} \tag{3.2-1}$$

$$G = \begin{pmatrix} 1 \\ 0 \\ 0 \end{pmatrix} \tag{3.2-2}$$

$$Q = \left(45 \frac{\beta^3 \sigma_N{}^2}{C_N{}^2}\right) \tag{3.2-3}$$

$$H = (0, 0, -V) \tag{3.2-4}$$

$$R = (\sigma_A{}^2 \Delta t) \tag{3.2-5}$$

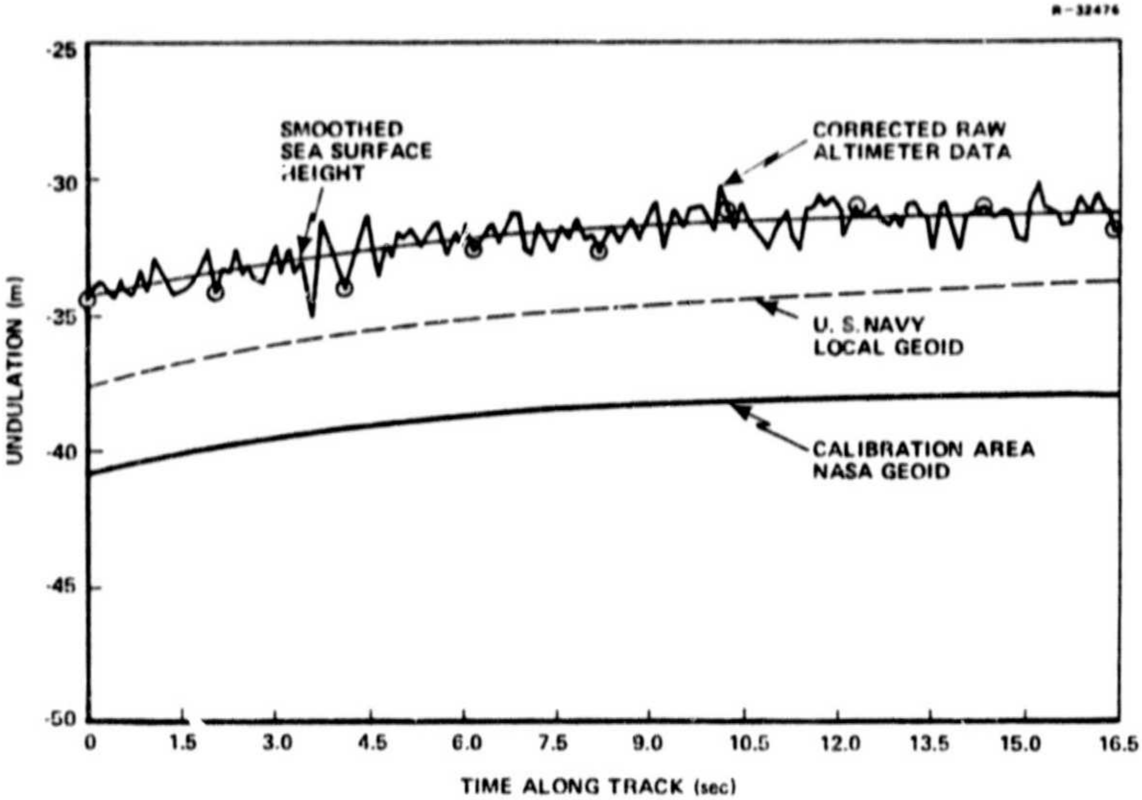

Figure 3.2-1 Comparison of Geoid Undulation Estimates (Rev. 2606)

where β=2.905 V/C_N, V is the GEOS-3 subtrack velocity (6.7 km/sec), Δt is the sampling interval (0.102405 sec), and σ_A is the altimeter noise (0.6m). For this model the undulation, N, is defined by

$$N = -Vx_3 \tag{3.2-6}$$

and the along track deflection of the vertical, λ, is given by

$$\lambda = \dot{x}_3 = x_2 - \beta x_3 \tag{3.2-7}$$

The data processing was preceded by the preprocessing and linear trend removal described earlier.

3.3 VERTICAL DEFLECTION ESTIMATION RESULTS

The results of the estimation of the along-track component of the vertical deflection for the tracks collected in the Blake Escarpment area were also compared to the vertical deflections calculated from the Navy survey data and interpolated along the satellite subtracks. The along track vertical deflection is given by the negative of the derivative of the undulation with respect to arc length along the track. Thus, the bias or long wavelength errors described earlier do not significantly affect the estimation of the vertical deflections. Of course, linear trends in the long wavelength errors would directly affect the vertical deflection estimates. However, these long wavelength slopes should not exceed 0.25 $\widehat{sec}$. Assuming an orbit determination accuracy of radial velocity of better than 1 cm/sec.

Typical results of the vertical deflection comparison show insignificant mean differences between the estimates produced from the GEOS-3 data and those estimates derived from the Navy data. The rms differences were typically between one and two $\widehat{sec}$. Significant mean differences (2-5 $\widehat{sec}$.) can arise over significant ocean currents like the Gulf Stream, and this must be considered when evaluating the results. Gulf Stream information was obtained from the Department of Commerce and NAVOCEANO for use in determining the current velocities and boundaries in order to correct for sea surface slope according to the geostrophic approximation (Ref. 11).

The results of the vertical deflection comparison performed for Rev. 2606 are presented in Fig. 3.3-1. This portion of the track did not overlap a significant part of the Gulf Stream. The vertical deflections estimated from the altimeter data were produced using optimal Kalman smooth-

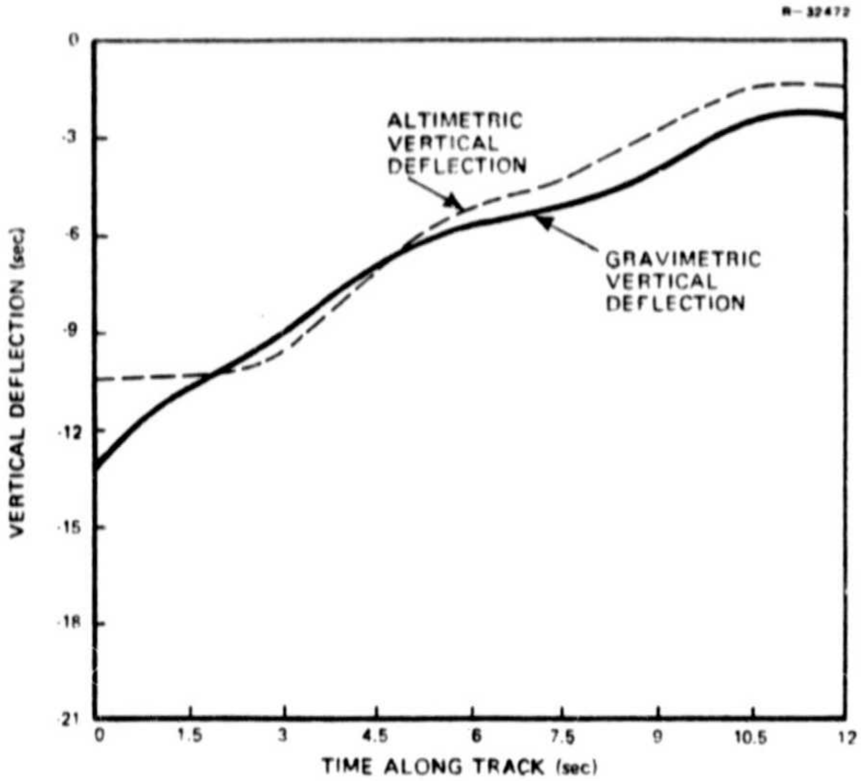

Figure 3.3-1 Comparison of Vertical Deflection Estimates (Rev. 2606)

ing and the model defined in Eqs. 3.2-1 through 3.2-7. The vertical deflections estimated from the Navy ocean survey data were produced from a numerical integration of the Vening-Meinesz equations and a spline function interpolation along the satellite subtrack.

4. GEOID RESOLUTION CAPABILITY OF THE GEOS-3 SATELLITE ALTIMETER

4.1 APPROACHES TO THE GEOID RESOLUTION PROBLEM

The analysis of the previous section has produced estimates of rms errors. It is the purpose of this section to extend this analysis by determining geoid wavelengths that can be reliably resolved from the altimeter data. The emphasis in this analysis is on short (less than 100 km) wavelength resolution. Of course, long wavelength resolution is also of interest for related studies, and this resolution is limited by coverage and orbit errors. However, the focus of the work described here is on the short wavelength resolution problem.

Short wavelength geoid resolution by satellite altimeters could potentially be limited by many factors including along-track sampling rate, altimeter beam spot size, effective signal to noise ratio (ratio of geoid to altimeter noise power) and short wavelength ocean surface effects (currents, sea state). The results shown in this section indicate that the limiting factor for the GEOS-3 data is the effective signal to noise ratio. Thus, it is likely that in regions other than the Blake Escarpment area, the lower bounds on the geoid wavelengths resolvable in the data would be higher or lower depending on whether or not there was less or more power in the short wavelength geoid variations.

In analyzing the resolution capability of the GEOS-3 altimeter, two approaches were adopted, neither of which relies necessarily on the use of parametric models, as discussed in Section 3.1. The first of these approaches, described in Section 4.2, is based on the spectrum analysis of single tracks of data. While this is obviously not an optimum approach to estimating the altimeter resolution due to the relatively small amount of data involved, it can provide some useful insights and approximate answers. The second approach involves the simultaneous analysis of groups of closely spaced parallel subtracks and the quantitative assessment of the repeatability of each wavelength in the data. The quantitative assessment is based on the estimation of the spectral coherence function (Ref. 12) which is effectively the squared correlation coefficient of the data along two subtracks at each frequency (or wavelength) in the altimetry data spectrum.

Given two stationary stochastic processes, x and y, the cross-correlation function is defined by

$$C_{xy}(\tau) = E\left[x(t)\ y(t+\tau)\right] \tag{4.1-1}$$

where E $(\cdot)$ is the expectation operator. The cross-spectrum, $S_{xy}(\omega)$, is the Fourier transform of $C_{xy}(\tau)$

$$S_{xy}(\omega) = \int_{-\infty}^{\infty} C_{xy}(\tau) e^{-i\omega\tau} d\tau \tag{4.1-2}$$

The coherence spectrum, $\rho(\omega)$, is the normalized cross-spectrum defined by

$$\rho(\omega) = \frac{|S_{xy}(\omega)|^2}{S_{xx}(\omega) S_{yy}(\omega)} \tag{4.1-3}$$

As can be readily seen from Eq. 4.1-3, $0 \leq \rho(\omega) \leq 1$. The coherence function measures the correlation at each frequency. The application of this function to the estimation of geoid resolution is discussed in Section 4.3.

4.2 SPECTRUM ANALYSIS OF SINGLE GEOS-3 DATA TRACKS

This section describes typical results obtained from a spectrum analysis of GEOS-3 altimetry data over a subtrack arc length of approximately 1000 km. The analysis is performed on the data as a time series (i.e., data sampled uniformly in time), and interpreted in terms of physical wavelength using the fact that over limited regions the satellite subtrack is essentially linear with constant subtrack velocity. This is, of course, an approximation which is believed to be sufficiently accurate for the analysis described here, but no detailed error analysis has, as yet, been performed.

Short wavelength gravity anomalies are primarily due to ocean floor topography and to associated compensation at the Moho. Ocean surface gravity anomalies are influenced by the depth of the ocean in the following way. Consider a gravity anomaly spectrum on the ocean floor at the mean depth, h, given by $\Delta_o g(\omega_x,\omega_y)$ where ω_x and ω_y are the frequency variables in a local cartesian coordinate system (planar approximation). The anomaly spectrum at the surface, $\Delta_h g(\omega_x, \omega_y)$, is given by (Ref. 13) the equation

$$\Delta_h g(\omega_x,\omega_y) = e^{-h(\omega_x^2 + \omega_y^2)^{\frac{1}{2}}} \Delta_o g(\omega_x,\omega_y) \tag{4.2-1}$$

The geoid undulation spectrum, $N(\omega_x,\omega_y)$, is related to the gravity anomaly spectrum through the Stokes's transfer function (planar approximation) as follows

$$N(\omega_x,\omega_y) = \frac{1}{g_o(\omega_x{}^2 + \omega_y{}^2)^{\frac{1}{2}}} \Delta g(\omega_x,\omega_y) \tag{4.2-2}$$

The spectrum for a one-dimensional track is given by the integral of the two dimensional spectrum over the orthogonal frequency axis. For example,

$$N(\omega_x) = \int N(\omega_x, \omega_y) d\omega_y \qquad (4.2\text{-}3)$$

Under the assumption that $\Delta_o g(\omega_x, \omega_y)$ is bounded, it follows that the one dimensional spectrum $N(\omega_x)$ has the asymptotic form in sufficiently short wavelengths

$$N(\omega_x) \sim \frac{1}{\omega_x^{\frac{1}{2}}} e^{-h\omega_x} \qquad (4.2\text{-}4)$$

Accordingly, an approximately exponential character of the spectrum is anticipated in short wavelengths. It should be noted that the value of the parameter h that may be inferred from the spectrum may be larger than the ocean depth since the topography spectrum is not white and since the gravity anomalies may arise from deeper sources. Thus, the spectrum $\Delta_o g(\omega_x, \omega_y)$ may itself have an exponential character.

The exponential character of the spectrum will be dominated in very short wavelengths by other phenomena in the altimeter data. These include altimeter noise and other short wavelength phenomena which dominate the geoid power in sufficiently short wavelengths and form a relatively flat portion of the spectrum called the "noise floor". For accurate estimation of a signal of unknown form, a positive signal to noise ratio (SNR) of at least a factor of 3 to 5 is required. Accordingly, one simple way of estimating the geoid resolution capability of the altimeter is to observe the wavelength at which the SNR becomes negative. Due to the variance in the above sense does not have high precision, but, since the estimate is straightforward to produce, it is useful in a preliminary investigation.

The above discussion is illustrated in Fig. 4.2-1 which shows the power spectrum calculated for a segment of GEOS-3 Rev. 1810. The resolution bound for this data set is approximately 60 km as indicated in the figure.

This could be improved slightly by averaging the sea surface height values from a few closely-spaced subtracks which would have the effect of lowering the noise floor. This approach is limited by several factors. First, the number of available subtracks that are sufficiently close (e.g. 1-3 km) to average without distorting the signal process is limited, in the data currently available, to not more

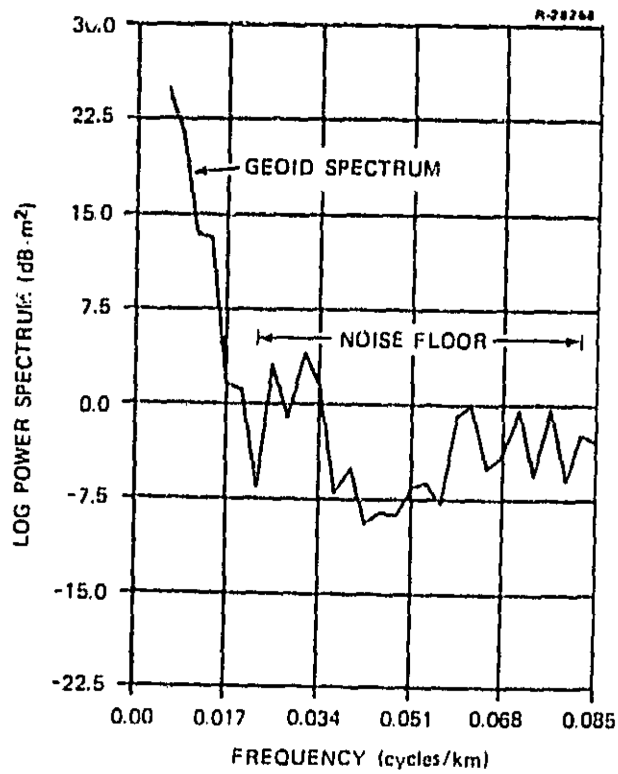

Figure 4.2-1 Sea Surface Height Power Spectrum (Rev. 1810)

than four. Thus, a reduction in the noise floor level can not exceed a factor of two. Second, the short wavelength disturbances are not purely uncorrelated altimeter noise and, thus, the ideal variance reduction may not be achieved in practice. Third, the signal spectrum is steep in this frequency range, and a small improvement in SNR will not lead to a significant increase in resolution. For example, an improvement by a factor of four in the case of Fig. 4.2-1, would change the approximate resolution bound from 60 km to 50 km.

Based on these preliminary results, it appears that the most important factors in achieving a higher geoid resolution are a lowering of the noise floor and increased track repeatability. A more systematic procedure for analyzing the resolution capability is also required. An approach to meeting this requirement is described in the next section.

4.3 CROSS-SPECTRUM ANALYSIS OF CLOSELY-SPACED PARALLEL SUBTRACKS

An alternate approach to estimating the geoid resolution capability of the altimeter is based on the assumption that repeatable components in the short wavelength variations present in the sea surface height data are due to geoid variations and not to ocean surface effects or altimeter noise. Since the tracks contained in Fig. 2.1-1 were collected over a period of many months, and at uncorrelated times during the day, the assumption seems reasonable.

Two possible objections, however, may be raised. First, the orbit determination errors will not be totally uncorrelated since the orbits for the closely-spaced tracks will be influenced by the same geopotential errors (Ref. 14). However, these effects will not influence the wavelengths considered here. The second objection is that altimeter errors may not be totally uncorrelated with the local geoid structure. Some evidence for this has already been shown in Fig. 2.2-1. This question requires further study, but the data analysis performed during this study indicates that the recurrence of spikes of other altimeter errors did not result in significant correlation after preprocessing in the short wavelengths indicated by their occurrence in the data. This will be shown in the coherence spectra described below.

Though the estimation of coherence need not be based on parametric models, satisfactory results were obtained by fitting vector autoregressive models of the form in Eq. 3.1-3 to segments of data along two closely spaced subtracks. The coherence spectrum can be readily calculated from the spectral density matrix based on the autoregressive model given by

$$S(\omega) = \left[I - \sum_{j=1}^{k} A_j \, e^{ij\omega} \right]^{-1} P \left[I - \sum_{j=1}^{k} A_j \, e^{-ij\omega} \right]^{-1} \qquad (4.3\text{-}1)$$

The auto-spectra required by Equation 4.1-3, are given by the diagonal elements of Equation 4.3-1, and the cross-spectra are given by the off-diagonal elements.

The statistical significance of a given level of coherence depends on the length of the data set, the accuracy of the data, samples, and the structure of the model which, in the cases considered here, is determined by the autoregression order. Statistical significance calculations in parametric models are discussed in (Ref. 12).

As noted earlier, the data collected along the nearly repeating subtracks exhibits high repeatability in the long wavelengths. This is illustrated in Fig. 4.3-1 which shows the smoothed sea surface height data along segments of Revs. 1810, 2336, and 2862. The relative bias-like offsets of the data are due to radial orbit determination error. It is likely that these biases are correlated due to geopotential errors, and that all three tracks have a common error (Ref. 14). It should also be noted that the subtracks for Revs. 2336, and 2862 are somewhat closer to each other than to the track for Rev. 1810, and this is reflected in a higher repeatability of the data. This higher repeatability is quantified by the coherence spectrum. For example, the estimated coherence between the data for Revs. 2336 and 2862 at a wavelength of 75 km is approximately 0.36. However the estimated coherence between the data for Revs. 1810 and 2336 at a wavelength of 75 km is only 0.20. Despite the qualitative similarity of the smoothed data, these sets are not highly coherent at short wavelengths.

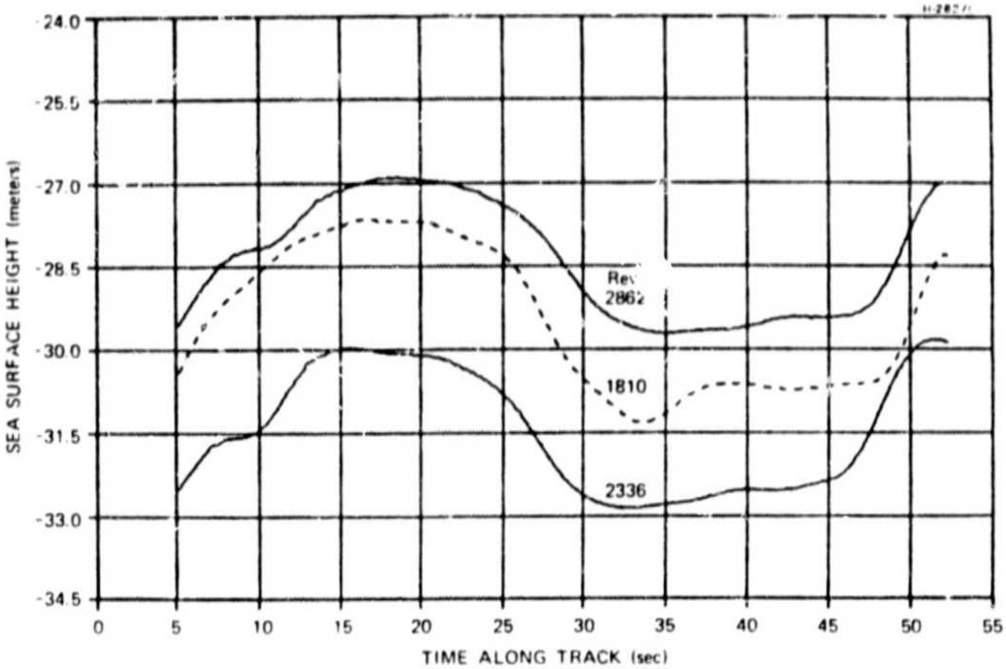

Figure 4.3-1 Smoothed Sea Surface Height Data for Revs. 1810, 2336, and 2862

A more representative example is given by Revs. 1682 and 3260. The raw data collected along these tracks is shown in Fig. 2.2-1. After preprocessing, the autoregressive model fitting program selected order 10 as the optimal order. Based on the tenth order order model, the coherence spectrum showed statistically significant coherence (95% confidence) down to wavelengths of 50 km. The coherence spectrum is shown in Fig. 4.3-2.

Similar analysis for the other tracks shown in Fig. 2.1-1 shows geoid resolution estimates based on significant coherence at wavelengths ranging from 30 km to 80 km. Had more tracks been available at sufficiently close spacing,

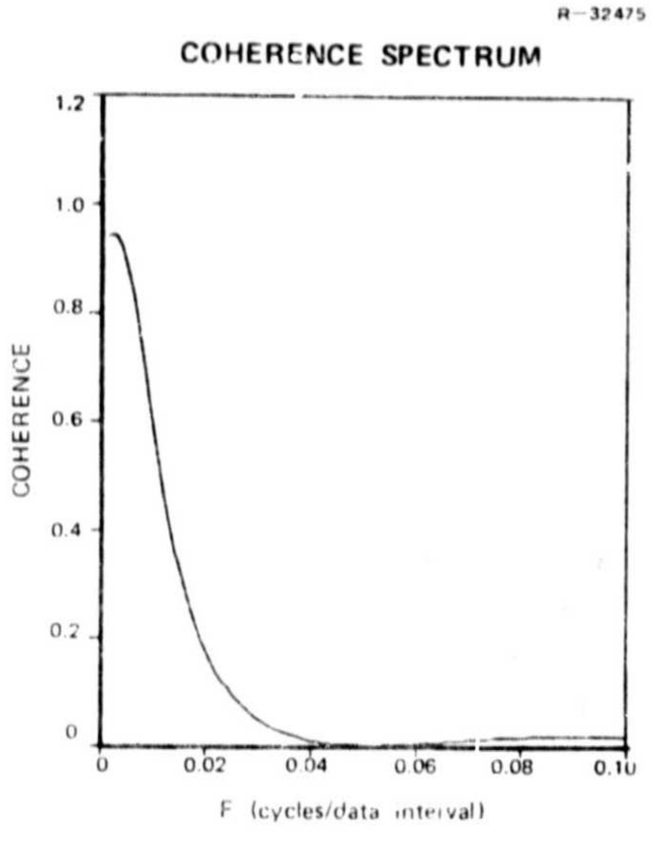

Figure 4.3-2 Coherence Spectrum for GEOS-3 Revs. 1682 and 3260

some averaging could have been performed, as discussed in Section 4.2, to increase the resolution before calculating the coherence. However, as noted as in Section 4.2, unless a large number of tracks were available (not currently the situation), the resolution estimate would not be significantly different. Thus, it can be seen from the preceding analysis that the GEOS-3 altimeter was able to resolve geoid features having wavelengths approximately 50 km in the region near the Blake Escarpment.

5. PRINCIPAL CONCLUSIONS

Based on the results of this study, the following principal conclusions may be drawn. These conclusions are based on data collected in the area near the Blake Escarpment.

- The geoid undulation accuracy as measured by the satellite altimeter is approximately 1 to 2 meters (rms). This conclusion is based on a comparison with geoid estimates produced from U.S. Navy shipboard survey data. Further confirmation of this result has come from comparison with results produced at other organizations (Ref. 9). The predominant error source is radial orbit determination error.

- Similar comparisons show that vertical deflections may be estimated to within an accuracy of 2 $\widehat{\text{sec}}$ (rms).

- The altimeter is capable of resolving geoid features having wavelengths as short as 30 km to 80 km.

The results of this study demonstrate that the GEOS-3 radar altimeter experiment was highly successful in providing accurate data for use in estimating the ocean geoid. Though the results of this study were obtained only for the Blake Escarpment region, it is highly probable that similar results can be obtained in the balance of the broad ocean areas covered by GEOS-3.

REFERENCES

1. Brammer, R.F. and Jordan, S.K., "Preliminary Results of GEOS-3 Altimetry Data Processing for Estimation of Local Undulations and Vertical Deflections," GEOS-3 Investigators Conference, NASA/Wallops Flight Center, Virginia, May 1976.

2. Martin, C.F. and Butler, M.L., "Calibration Results for the GEOS-3 Altimeter," NASA/Wallops Flight Center, Virginia, Report No. NASA CR-141430, September 1977.

3. Mofjeld, H.O., "Empirical Model for Tides in the Western Atlantic Ocean," NOAA, U.S. Department of Commerce, Boulder, Colorado, Report No. TR-ERL 340-AOML 19, October 1975.

4. Rabiner, L.R. and Gold, B., Theory and Application of Digital Signal Porcessing, Prentice-Hall Inc., New Jersey, 1975.

5. Gelb, A., ed., Applied Optimal Estimation, The M.I.T. Press, Cambridge, 1974.

6. Jordan, S.K., "Self-Consistent Statistical Models for the Gravity Anomaly, Vertical Deflections, and Undulation of the Geoid," Journal of Geophysical Research, Vol. 77, No. 20, July 1972.

7. Burg, J.P., "Maximum Entropy Spectral Analysis," Ph.D. Thesis, Department of Geophysics, Stanford University 1975.

8. Akaike, H., "Information Theory and an Extension of the Maximum Likelihood Principle," in Proc. 2nd Int. Symp. Information Theory, Supp. to Problems of Control and Information Theory, 1972, pp. 267-281.

9. Chappell, A., Naval Surface Weapons Center, Dahlgren Laboratory, private communication, October 1977.

10. Marsh, J.G. and Chang, E.S., "5' Detailed Gravimetric Geoid in the Northwestern Atlantic Ocean," Annual Fall Meeting, American Geophysical Union, San Francisco, California, December 1976.

11. Leitao, D.D., Parra, C.G., and Huang, N.E., "Measurements of the Gulf Stream by Geos-3 Radar Altimeter," Annual Spring Meeting, American Geophysical Union, Washington, D.C., May 1977.

12. Koopmans, L.H., The Spectral Analysis of Time Series, Academic Press, New York, 1974.

13. Grant, F.S. and West, G.F., Interpretation Theory In Applied Geophysics, McGraw-Hill Book Company, 1975.

14. Anderle, R.J., and Hoskin, R.L., "Correlated Errors in Satellite Altimetry Geoids," Geophysical Research Letters, Vol. 4, No. 10, October 1977.